ADVANCES IN NUCLEAR SCIENCE AND APPLICATIONS

Volume 1, No. 4 (2025), P. 269-284

# Empirical formulas for fragmentation production cross section

S.M. Lukyanov[1,*], V.A. Maslov[1], D. Aznabayev[1], T. Issatayev[1,2], K. Mendibayev[1,2], A.V. Shahov[1]

[1]Joint Institute for Nuclear Research, Dubna, Russia

[2]Institute of Nuclear Physics, Almaty, Kazakhstan

e-mail: lukyan@jinr.ru

DOI: 10.63907/ansa.v1i4.63
Received: 21 October 2025

**Abstract**

Production cross sections of neutron-rich nuclei in projectile fragmentation reactions measured at zero degrees are systematically analyzed using published experimental data. By comparing the yields of O, F, Ne, Na, Mg, Al, Si, and P isotopes produced in $^{40}$Ar-induced fragmentation at beam energies of 35 MeV/nucleon, 57–120 MeV/nucleon, and 1 GeV/nucleon, we demonstrate that the production cross sections of neutron-rich fragments are, within experimental uncertainties, essentially independent of the projectile energy over this broad range. Motivated by this limiting-fragmentation behavior, we propose an empirical systematics for neutron-rich fragment production based on the binding energy per nucleon ( BE/$A$ ) of the final nuclei. The cross sections are found to follow a steep exponential dependence on BE/$A$, spanning 8–9 orders of magnitude for small variations of BE/$A$. The systematics is tested for reactions induced by $^{40}$Ar, $^{48}$Ca, $^{58,64,68}$Ni, $^{72}$Zn, $^{76}$Ge, $^{82}$Se, and $^{86}$Kr projectiles on Be and Ta targets, and the corresponding fit parameters are shown to correlate with the fragment charge $Z$ and the projectile neutron-to-proton ratio $(N/Z)_{\text{projectile}}$. Additionally, a complementary analysis based on $Q_{gg}$ systematics (mass difference between projectile and detected fragments) is also presented, and the advantages and limitations of the BE/$A$-based description for extrapolating yields toward the neutron drip line are discussed.

# 1 Introduction

Deep-inelastic transfer reactions [1] and projectile fragmentation [2] have long been recognized as the most effective mechanisms for the production of exotic nuclei far from the valley of stability. These reaction mechanisms are widely exploited at major radioactive-beam facilities, including GANIL (France) [3, 4], the NSCL at Michigan State University (USA) [5, 6], Flerov Laboratory of Nuclear Reaction (JINR, Dubna) and RIKEN (Japan) [7]. Beams of accelerated radioactive nuclei provide access to nuclear systems with extreme neutron-to-proton ratios, enabling both the synthesis of new neutron-rich isotopes and detailed investigations of their structural and decay properties, which may differ substantially from those of stable nuclei. In addition, reactions induced by projectiles with anomalous $N/Z$ ratios offer valuable insight into the underlying dynamics of heavy-ion reactions.

Early experiments carried out at Dubna using $^{22}$Ne and $^{40}$Ar beams at energies below 10 MeV/nucleon resulted in the production of approximately twenty previously unknown isotopes located far from the line of stability [1]. These studies led to the identification of a new reaction mechanism involving heavy ions, later termed deep-inelastic transfer reactions. This mechanism represents an intermediate process between complete fusion and direct reactions and was extensively investigated at energies up to 10 MeV/nucleon. It was demonstrated that isotope yields in deep-inelastic processes can be successfully described in terms of reaction energetics, including shell effects, within the framework of the $Q_{gg}$ systematics.

For a long time, progress toward the neutron drip line using deep-inelastic transfer reactions was believed to be severely limited by the rapidly decreasing production cross sections of the most neutron-rich isotopes. This limitation stimulated the exploration of heavy-ion reactions at higher energies, where projectile fragmentation on thick targets enables the production of a large number of neutron-rich light nuclei with comparatively high cross sections. With increasing projectile energy, fragmentation becomes the dominant reaction mechanism. At intermediate and relativistic energies, projectile fragmentation has therefore evolved into a well-established method for producing rare isotopes [3, 4]. At the same time, multinucleon transfer reactions continue to be actively discussed as a complementary approach for accessing neutron-rich nuclei.

In deep-inelastic transfer reactions, the excitation energy imparted to the reaction products is typically smaller than in fragmentation reactions. In contrast, high-energy fragmentation processes generally populate highly excited prefragments, which subsequently undergo statistical de-excitation. While microscopic descriptions of high-energy fragmentation often rely on computationally intensive Monte Carlo simulations, an important advantage of analytical parameterizations lies in their computational efficiency and their ability to provide rapid estimates of production cross sections. In this context, Summerer *et al.* [8] introduced the semiempirical EPAX parameterization for projectile fragmentation cross sections. The original formulation of EPAX was largely based on proton-induced fragmentation data at energies of several GeV, reflecting the limited availability of heavy-ion fragmentation data at the time.

Subsequent experimental studies have shown that fragmentation induced by relativistic heavy ions generally deposits more excitation energy into the system than proton-induced reactions, resulting in broader isotope distributions with a stronger

neutron deficit after evaporation. Nevertheless, experimental data indicate that, in both cases, isotope yield distributions can be well described by simple analytical functions, often resembling Gaussian shapes with smoothly varying mass-dependent parameters. In the fragmentation process, the sequential evaporation of light particles from highly excited nuclei leads to relatively smooth final isotope distributions, which are successfully reproduced by the EPAX systematics based on a large body of high-energy experimental data [8]. The underlying reaction dynamics bear similarities to deep-inelastic transfer processes: the kinetic energy associated with the relative motion of the colliding nuclei is rapidly converted into internal excitation energy, leading to the formation of a dinuclear system in which nucleon diffusion may occur. To preserve a neutron excess, the emerging prefragments must remain sufficiently cold; otherwise, neutron evaporation during de-excitation drives the system toward more neutron-deficient secondary products.

The applicability of the EPAX formalism is subject to several important limitations. First, in the absence of systematic excitation-function measurements for heavy-ion-induced fragmentation, the parameterization is expected to be valid primarily in the so-called limiting-fragmentation regime, where fragment yields become effectively independent of projectile energy within the intrinsic uncertainty of the model, typically within a factor of two. This condition is generally satisfied for beam energies well above the Fermi energy in nuclei, i.e., above approximately 40 MeV/nucleon. Second, EPAX is designed mainly for the fragmentation of medium-mass and heavy projectiles and does not explicitly account for nucleon transfer processes or fission of the produced fragments. The isotope distributions are therefore assumed to be governed predominantly by the statistical evaporation of highly excited fragments formed in relativistic heavy-ion collisions.

However, the EPAX parameterization does not explicitly consider the possible formation of a dinuclear system with limited nucleon diffusion between the target and projectile. Experimental evidence indicates that even at relatively high beam energies, transfer-like processes can make a significant contribution. For example, in reactions induced by $^{48}$Ca beams at 55 MeV/nucleon, new isotopes such as $^{44}$P, $^{45–47}$S, $^{46–49}$Cl, and $^{49–51}$Ar, with neutron numbers $N \geq 28$ exceeding that of the projectile, were observed for the first time [3]. At even higher energies of 144 MeV/nucleon, additional neutron-rich isotopes, including $^{40}$Mg, $^{42,43}$Al, and $^{44}$Si, were produced [9]. Moreover, theoretical studies suggest that multinucleon transfer reactions may yield production cross sections for certain exotic nuclei that are comparable to, or even exceed, those obtained in high-energy fragmentation reactions, despite the lower experimental collection efficiency typically associated with transfer processes [10].

Systematic studies of projectile fragmentation over a wide range of beam energies have established a solid experimental basis for the production of neutron-rich nuclei [11, 12, 13, 14, 15]. These measurements demonstrated the approximate energy invariance of isotopic production cross sections measured at zero degrees and provided detailed information on fragment yield systematics. Subsequent experimental investigations extended these studies to different projectile–target combinations and increasingly neutron-rich systems [16, 17, 18, 19, 20], as well as to more recent high-precision measurements with stable and radioactive beams [21, 22, 23, 24, 25], confirming that projectile fragmentation remains a robust and well-established reaction mechanism and that the statistical de-excitation picture provides a consistent

description of neutron-rich fragment production.

Existing parameterizations such as EPAX provide global descriptions of fragmentation yields but do not explicitly incorporate the binding properties of the final nuclei, while $Q_{gg}$-based systematics depend on model assumptions and on the knowledge of masses of unobserved reaction partners. This motivates the development of alternative systematics based solely on intrinsic properties of the produced fragments. The present work provides a systematic validation of the approximate energy invariance of neutron-rich fragment production cross sections measured at zero degrees over a broad projectile-energy range from 35 MeV/nucleon up to 1 GeV/nucleon, based on a unified analysis of published experimental data. Using fragmentation data induced by $^{40}$Ar, $^{48}$Ca, $^{58,64,68}$Ni, $^{72}$Zn, and $^{86}$Kr projectiles, we demonstrate that, within experimental uncertainties, the production cross sections of neutron-rich nuclei exhibit no significant dependence on the incident projectile energy in this range. Motivated by this observation, we develop an empirical systematics for projectile fragmentation yields expressed in terms of the binding energy per nucleon of the final nuclei. The parameters of the resulting exponential dependence are shown to exhibit regular and physically meaningful correlations with the fragment charge and with the neutron-to-proton ratio of the projectile. The proposed parameterization is tested for a wide range of projectile–target combinations, compared with existing approaches based on $Q_{gg}$ systematics and the EPAX formalism, and its applicability and limitations for describing and extrapolating neutron-rich fragment yields are discussed.

## 2 Experimental evidence for the energy invariance of neutron-rich fragment production cross sections in fragmentation

Figure 1 presents the production cross sections of O, F, Ne, Na, Mg, Al, Si, and P isotopes obtained in projectile fragmentation of a $^{40}$Ar beam at different incident energies [7], [11], [12], [13]. The targets used in the experiments analyzed in the present work were of natural isotopic composition. For light (Be) and heavy (Ta) targets, the influence of the specific isotopic composition on the production cross sections of projectile fragmentation products measured at zero degrees is negligible compared to the experimental uncertainties. Therefore, the isotopic composition of the targets is not explicitly taken into account in the present systematics. For comparison, the corresponding cross sections calculated using the EPAX parameterization are also shown. For isotopes located close to the valley of stability, some discrepancies between the experimental data and the EPAX calculations are observed; however, these differences are not the subject of the present work. Overall, the EPAX calculations reproduce the experimental cross sections in this region with reasonable accuracy. Within experimental uncertainties, the variation of the production cross sections does not exceed a factor of two over the energy range from 35 MeV/nucleon to 1 GeV/nucleon. The observed energy invariance at 35 MeV/nucleon is established empirically and does not imply a specific reaction mechanism, but rather reflects the robustness of zero-degree fragment yields.

Particular attention should be paid to the agreement of the experimental production cross sections of neutron-rich nuclei obtained at different $^{40}$Ar beam energies, as

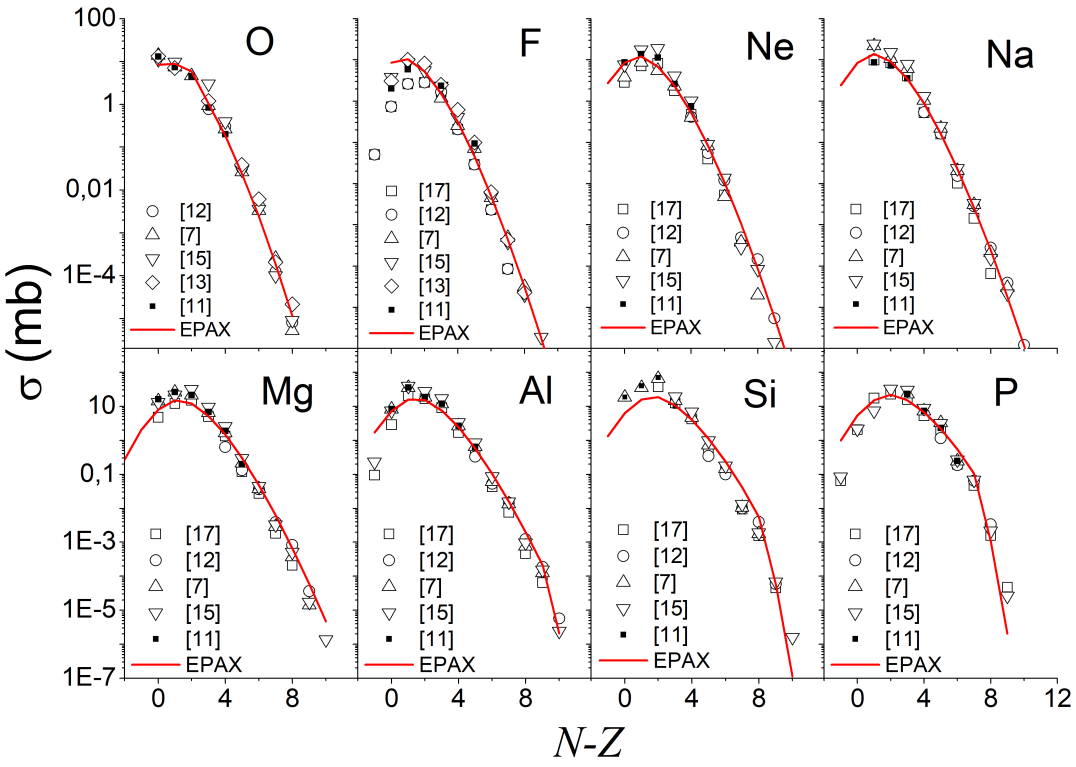


Figure 1: Production cross sections of O, F, Ne, Na, Mg, Al, Si, and P isotopes as functions of the neutron excess of the final products for fragmentation of an Ar beam on a Be target at different energies: 35 MeV/nucleon [11], 57 MeV/nucleon [12], 90 MeV/nucleon [7], 120 MeV/nucleon [12], and 1 GeV/nucleon [13]. The solid curve represents the results of calculations performed using the EPAX parameterization.

well as to the good overall consistency between the experimental data and the EPAX calculations. The main conclusion drawn from the dependencies shown in Figure 1 is that the production cross sections of neutron-rich fragments do not depend on the energy of the incident projectile. This conclusion holds over a broad energy range from 35 MeV/nucleon up to 1 GeV/nucleon. As follows from the figure, the production cross sections of neutron-rich isotopes exhibit nearly identical values in all considered cases.

Thus, the production cross sections of neutron-rich isotopes produced in reactions induced by $^{40}$Ar ions are in good agreement despite the substantial variation in the projectile energy. This observation provides further evidence that the production cross sections of such fragments are not governed by the projectile energy but are primarily determined by the intrinsic properties of the final nuclei. This result indicates that the fragmentation process is accompanied by strong de-excitation of the prefragments, leading to the formation of final products predominantly in their ground or weakly excited states. This finding serves as the experimental basis for the development of a new systematics of exotic nucleus production that depends on the properties of the produced fragments themselves.

# 3 Systematics of neutron-rich fragment production based on the binding energy $BE(Z, N)$

By definition, the $Q_{gg}$ systematics assumes a two-body reaction mechanism in the exit channel. However, this condition is not always fulfilled, since the produced prefragments are typically formed in excited states, and their de-excitation may be accompanied by the emission of nucleons, resulting in a reduction of the mass of the final products.

Moreover, in certain reactions, such as $^{48}$Ca+Be$\rightarrow^{29}$P, the associated unstable product $^{28}$F is formed, for which the mass value is not experimentally known. As a consequence, the dependence of the production cross sections on $Q_{gg}$ becomes model dependent.

In order to eliminate this model dependence, a $Q_{gg}$ systematics was proposed in Refs. [6, 7], in which the fragmentation cross sections are expressed as functions of the difference between the mass defects of the incident projectile and the detected reaction product.

## 3.1 Fragmentation cross sections and $BE(Z, N)$

In Refs. [16, 17, 18], a systematics of reaction cross sections based on the binding energy of the produced fragments was proposed. This approach is well justified, since, as discussed above, the production cross sections of neutron-rich nuclei are essentially independent of the incident projectile energy.

As a result of the interaction, statistical equilibrium is established, and the fragment yields are expected to depend primarily on the proton number $Z$, mass number $A$, and the effective slope parameter $\tau$ of the formed system. Under these assumptions, the fragment yield can be written as

$$Y(Z, N) = \text{Const} \exp\left[\frac{N\mu_n + Z\mu_p - F}{\tau}\right], \tag{1}$$

where $A = Z + N$, and $\mu_n$ and $\mu_p$ are the neutron and proton chemical potentials, respectively. The free-energy term $F$ is expressed as the sum of the ground-state contribution $E_0$ and the excitation contribution $F^*$, i.e., $F = E_0 + F^*$. The ground-state term is determined by the binding energy as $E_0 = -B(Z, N)$.

Within the Fermi-gas approximation, the excitation contribution can be approximated as

$$F \approx -0.5 \cdot \min(S_n, S_p, S_\alpha) + F_0(Z, N), \tag{2}$$

where $S_n$, $S_p$, and $S_\alpha$ are the separation energies of a neutron, proton, and $\alpha$ particle, respectively. The term $F_0(Z, N)$ accounts for pairing effects and is given by

$$F_0(Z, N) = \frac{1}{2}\left[(-1)^N + (-1)^Z\right] F_{p0} A^{3/4}. \tag{3}$$

Introducing the effective binding energy per nucleon $B' = \frac{B - \varepsilon_{\text{pair}}}{A}$, Eq. (1) can be rewritten in the form

$$\sigma = C \exp\left(\frac{B' - 8}{\tau}\right), \tag{4}$$

where $C$ and $\tau$ are parameters determined from the experimental data. Here $B'$ is the binding energy per nucleon of the detected fragment, and $\varepsilon_p$ is the pairing correction given by

$$\varepsilon_p = \frac{1}{2}\left[(-1)^N + (-1)^Z\right]\varepsilon A^{-3/4}, \tag{5}$$

with $\varepsilon = 30$ MeV [18, 19]. Expressing the yields in terms of the binding energy per nucleon allows one to factor out the trivial mass dependence and directly compare fragments with different $A$ and $Z$. As a result, a simplified expression for the production cross section is obtained:

$$\sigma = C_{\mathrm{BE}} \exp\left(\frac{(B - \varepsilon_{\mathrm{pair}})/A - 8}{\tau_{\mathrm{BE}}}\right), \tag{6}$$

where $C_{\mathrm{BE}}$ and $\tau_{\mathrm{BE}}$ are fitting parameters, and $(B - \varepsilon_{\mathrm{pair}})/A$ denotes the effective binding energy per nucleon of the observed fragment. The constant value of 8 MeV corresponds to a typical binding energy per nucleon of stable nuclei and is introduced to define a convenient reference scale for the exponential dependence; it does not represent an additional free parameter.

Figure 2 shows the production cross sections of O, F, Ne, Na, Mg, Al, Si, and P isotopes as functions of the binding energy per nucleon ( BE/$A$ ), obtained in projectile fragmentation of an Ar beam on a Be target at different energies: 35 MeV/nucleon [11], 57 MeV/nucleon [14], 90 MeV/nucleon [7, 15], 120 MeV/nucleon [12], and 1 GeV/nucleon [13]. The solid curve represents the result of a fit using Eq. (6). It is evident that the dependence of the production cross section on BE/$A$ is very steep: a relatively small variation of BE/$A$ in the range from 6 to 8 leads to changes in the cross sections by 8–9 orders of magnitude.

As follows from Figure 2, the production cross sections of neutron-rich isotopes are well described by an exponential dependence on the binding energy per nucleon according to Eq. (6). This result provides further confirmation that the production cross sections are independent of the projectile energy and are determined primarily by the intrinsic properties of the produced fragments.

## 3.2 Determination of the $C_{\mathrm{BE}}$ and $\tau_{\mathrm{BE}}$

Following the analysis of neutron-rich fragment production cross sections as functions of the binding energy per nucleon ( BE/$A$ ) for the $^{40}$Ar+Be reaction, a similar analysis was performed for reactions induced by $^{48}$Ca [19], $^{58,64}$Ni [19], $^{68}$Ni, $^{72}$Zn [20], and $^{86}$Kr [19]. For all these reactions, the parameters $C_{\mathrm{BE}}$ and $\tau_{\mathrm{BE}}$ of to Eq. (6) were extracted from fits to the experimental data. It should be emphasized that the parameters $\tau_{\mathrm{BE}}$ and $\tau_{Q_{gg}}$ introduced in the exponential parameterizations do not represent thermodynamic temperatures of the system. Rather, they should be regarded as effective slope parameters characterizing the steepness of the fragment yield distributions.

As can be seen from the corresponding systematics, the amplitude parameter $C_{\mathrm{BE}}$ is not only a function of the atomic number $Z$ of the detected fragment, decreasing systematically with increasing $Z$, but also depends on the neutron-to-proton ratio of the projectile, $(N/Z)_{\mathrm{projectile}}$. For a fixed value of $Z$, the largest values of $C_{\mathrm{BE}}$ are observed for the most neutron-rich projectiles, $^{48}$Ca and $^{72}$Zn,

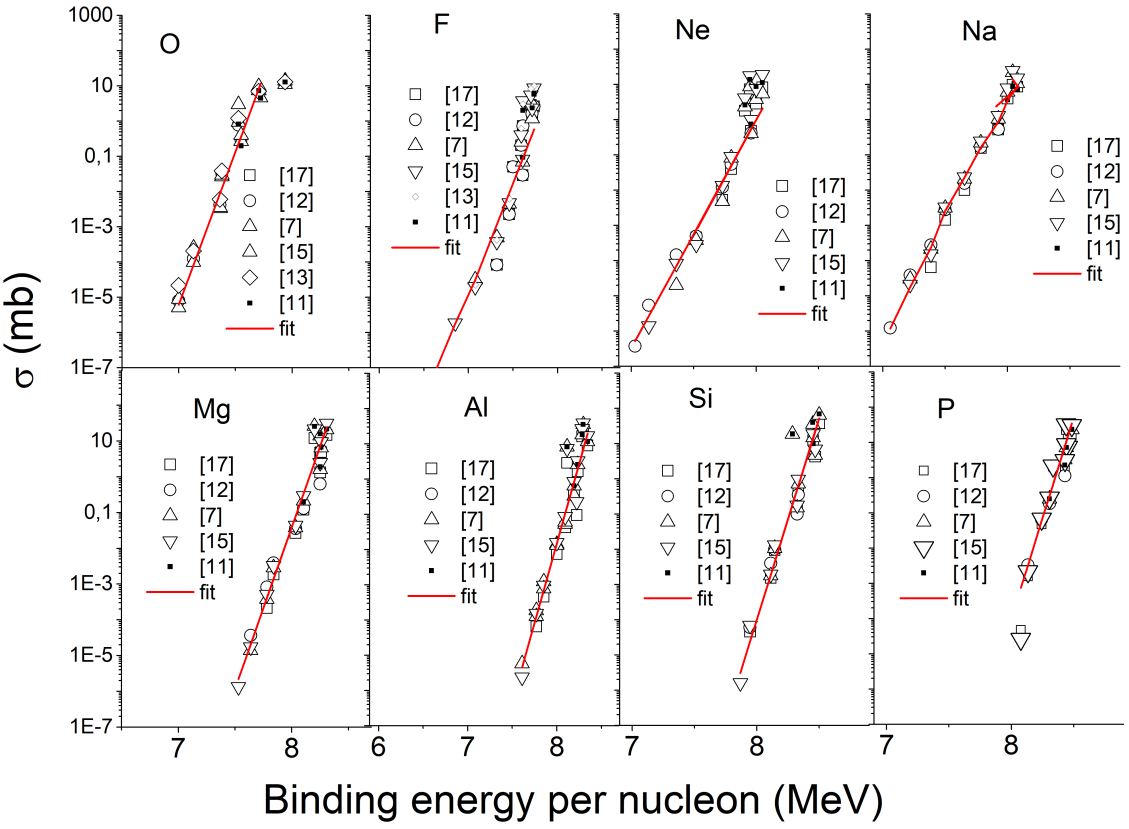


Figure 2: Production cross sections of O, F, Ne, Na, Mg, Al, Si, and P isotopes as functions of the binding energy per nucleon ( $\mathrm{BE}/A$ ), obtained in projectile fragmentation of an Ar beam on a Be target at different energies: 35 MeV/nucleon [11], 57 MeV/nucleon [14], 90 MeV/nucleon [7, 15], 120 MeV/nucleon [12], and 1 GeV/nucleon [13]. The solid curve represents the result of a fit using Eq. (6).

for which $(N/Z)_{\mathrm{projectile}} \approx 1.4$. In contrast, the smallest values of $C_{\mathrm{BE}}$ correspond to projectiles such as $^{40}$Ca with $(N/Z) = 1$ and $^{58}$Ni with $(N/Z)_{\mathrm{projectile}} = 1.07$.

For projectiles such as $^{40}$Ar and $^{64}$Ni, both characterized by $(N/Z)_{\mathrm{projectile}} \approx 1.24$, the dependence of $C_{\mathrm{BE}}$ on the fragment charge $Z$ is nearly identical over the entire range $10 \leq Z \leq 20$. In the case of the $^{86}$Kr projectile [19], with $(N/Z)_{\mathrm{projectile}} = 1.35$, the $C_{\mathrm{BE}}(Z)$ dependence was extracted for fragments with $Z \gtrsim 25$, whereas for $^{40}$Ar and $^{64}$Ni this dependence was obtained for lower $Z$ values. Despite these differences in the accessible $Z$ ranges, the $C_{\mathrm{BE}}(Z)$ dependence for the $^{40}$Ar and $^{64}$Ni reactions smoothly continues the corresponding trend observed for the $^{86}$Kr-induced reaction with a similar projectile $(N/Z)$ ratio. A similar regularity is observed for the reactions induced by $^{48}$Ca and $^{72}$Zn. These observations indicate that the amplitude parameter can be expressed as a function

$$C_{\mathrm{BE}} = f((N/Z)_{\mathrm{projectile}}, Z)\,. \tag{7}$$

The dependence of the effective slope parameter $\tau_{\mathrm{BE}}$, obtained from fits using Eq. (6), is shown in Figs. 4 and 5 for reactions $^{64}$Ni+Ta and $^{64}$Ni+Be [19], $^{48}$Ca+Ta and $^{48}$Ca+Be [19], $^{40}$Ar+Be [7], and $^{86}$Kr+Be [19]. A notable feature of these systematics is the presence of a local maximum in the region $Z > 20$ for fragments produced in reactions induced by $^{58,64}$Ni projectiles on Be and Ta targets, which is observed consistently in both the $C_{\mathrm{BE}}$ and $\tau_{\mathrm{BE}}$ dependencies.

As follows from Figure 3, the fragmentation cross sections depend on the properties of the incident projectile. To account for this dependence, a $Q_{gg}$ systematics was proposed in Refs. [6, 7], in which the production cross sections are expressed as functions of the difference between the mass defects of the projectile and the detected fragment.

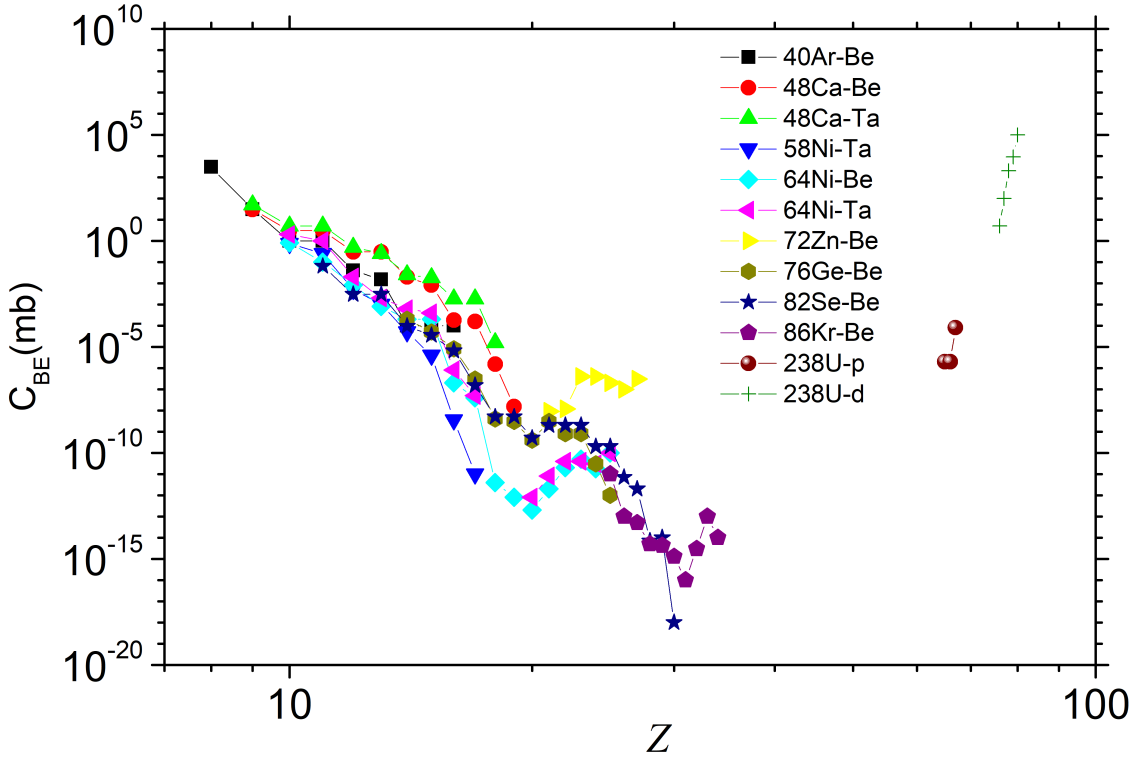


Figure 3: Dependence of the amplitude parameter $C_{\mathrm{BE}}$, extracted from fits to the isotope yields, on the atomic number $Z$ of the detected fragments for various reactions. Shown are results for $^{58}$Ni+Ta and $^{64}$Ni+Be [19], $^{48}$Ca+Ta and $^{48}$Ca+Be [19], $^{40}$Ar+Be [11], and $^{86}$Kr+Be [19]. Also included are data obtained with secondary beams in the reactions $^{68}$Ni+Be and $^{72}$Zn+Be [20], as well as results for proton- and deuteron-induced reactions on U targets at relativistic energies [2], and for the reaction $^{76}$Ge+Be at 132 MeV/nucleon [5].

Figure 4 shows the dependence of the fitting parameter $\tau_{\mathrm{BE}}$ on the atomic number $Z$ of the detected fragments for a wide range of projectile fragmentation reactions. The parameter $\tau_{\mathrm{BE}}$ was extracted from exponential fits of the production cross sections as functions of the binding energy per nucleon according to 6.

As can be seen from Figure 4, the parameter $\tau_{\mathrm{BE}}$ exhibits a systematic decrease with increasing fragment charge $Z$ for all considered reactions. For light and intermediate-mass fragments ($Z \approx 8$–$15$), $\tau_{\mathrm{BE}}$ typically lies in the range of 0.05–0.07 MeV, while for heavier fragments the values gradually decrease to $\tau_{\mathrm{BE}} \approx 0.02$–0.03 MeV. This behavior is observed consistently for different projectiles and targets, including reactions induced by $^{40}$Ar, $^{48}$Ca, $^{58,64}$Ni, $^{72}$Zn, $^{76,82}$Ge, and $^{86}$Kr ions.

For projectiles with similar neutron-to-proton ratios, such as $^{40}$Ar and $^{64}$Ni, the $\tau_{\mathrm{BE}}(Z)$ dependences closely follow each other over the entire overlapping $Z$ range. In contrast, more neutron-rich projectiles, notably $^{48}$Ca and $^{72}$Zn, tend to yield systematically higher values of $\tau_{\mathrm{BE}}$ at a given fragment charge. This observation

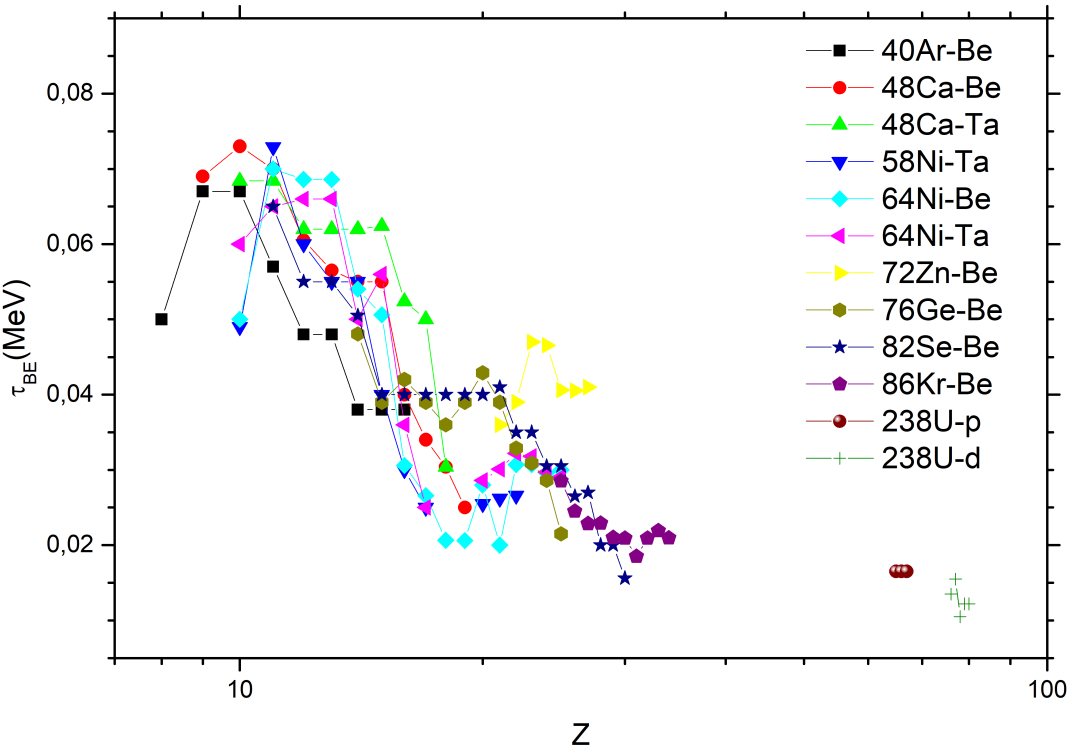


Figure 4: Dependence of the parameter $\tau_{\mathrm{BE}}$, extracted from fits to the isotope yields, on the atomic number $Z$ of the detected fragments for various reactions. Shown are results for $^{58}$Ni+Ta and $^{64}$Ni+Be [19], $^{48}$Ca+Ta and $^{48}$Ca+Be [19], $^{40}$Ar+Be [11], and $^{86}$Kr+Be [19]. Also included are data obtained with secondary beams in the reactions $^{68}$Ni+Be and $^{72}$Zn+Be [20], as well as results for proton- and deuteron-induced reactions on U targets at relativistic energies [2], and for the reaction $^{76}$Ge+Be at 132 MeV/nucleon [5].

indicates that the parameter $\tau_{\mathrm{BE}}$ is sensitive not only to the fragment charge but also to the neutron content of the projectile.

The data obtained with secondary beams, as well as results for proton- and deuteron-induced reactions on uranium targets at relativistic energies, fall within the same general systematics. Despite the substantial differences in reaction mechanisms and entrance channels, the extracted values of $\tau_{\mathrm{BE}}$ remain confined to a relatively narrow range and follow the same overall decreasing trend with $Z$. This suggests that $\tau_{\mathrm{BE}}$ reflects an effective de-excitation scale of the prefragments that is largely governed by the properties of the final nuclei.

Overall, the systematics presented in Figure 4 demonstrate that the binding-energy-based description provides a robust and physically meaningful parameterization of neutron-rich fragment production. Together with the observed behavior of the amplitude parameter $C_{\mathrm{BE}}$, these results support the interpretation of fragmentation as a process dominated by strong statistical de-excitation, leading to fragment yields that are primarily determined by the intrinsic properties of the produced nuclei.

# 4 Fragmentation cross sections and $Q_{gg}$

Figure 5, analogous to Figs. 1 and 2, shows the production cross sections of O, F, Ne, Na, Mg, Al, Si, and P isotopes as functions of $Q_{gg}$, obtained in projectile fragmentation of an Ar beam on a Be target at different energies: 35 MeV/nucleon [11], 57 MeV/nucleon [14], 90 MeV/nucleon [7, 15], 120 MeV/nucleon [12], and 1 GeV/nucleon [13].

As can be seen from Figure 5, the dependence of the fragmentation cross sections for neutron-rich nuclei on $Q_{gg}$, similar to the dependence on the binding energy per nucleon ($\mathrm{BE}/A$), can be described by an exponential function of the form

$$\sigma = C_{Q_{gg}} \exp\left(\frac{Q_{gg}}{\tau_{Q_{gg}}}\right), \tag{8}$$

in analogy with Eq. (6).

Using the parameterization given by Eq. (8), fragmentation cross sections were analyzed for a wide set of reactions, including $^{64}$Ni+Ta and $^{64}$Ni+Be [19], $^{58}$Ni+Ta, $^{72}$Zn+Be [20], and $^{86}$Kr+Be [19], as well as reactions induced by secondary beams. In addition, data for proton- and deuteron-induced reactions on U targets at relativistic energies [2], and for the reaction $^{76}$Ge+Be at 132 MeV/nucleon [5], were included in the analysis.

Based on this systematic study of the available experimental cross sections, the parameters $C_{Q_{gg}}$ and $\tau_{Q_{gg}}$ were extracted for the considered reactions. Figure 6 shows the dependence of these parameters on the atomic number $Z$ of the detected isotopes.

Figure 6 illustrates the dependence of the fitting parameter $C_{Q_{gg}}$ on the atomic number $Z$ of the detected fragments for a broad set of reactions induced by heavy ions, as well as by protons and deuterons at relativistic energies. As shown in Figure 6(b), for projectile fragmentation reactions induced by $^{40}$Ar, $^{48}$Ca, $^{58,64}$Ni, $^{72}$Zn, $^{76,82,86}$Ge, and $^{86}$Kr projectiles on Be and Ta targets, the parameter $C_{Q_{gg}}$ exhibits a clear systematic decrease with increasing fragment charge $Z$. This behavior is observed over several orders of magnitude and persists despite significant differences in projectile mass, neutron-to-proton ratio, and incident energy.

The data demonstrate that, for projectiles with similar $(N/Z)_{\mathrm{projectile}}$ ratios, the $C_{Q_{gg}}(Z)$ dependences follow closely related trends. In particular, reactions induced by $^{40}$Ar and $^{64}$Ni projectiles show nearly identical $C_{Q_{gg}}(Z)$ systematics over the overlapping $Z$ range, consistent with their comparable neutron excess. In contrast, more neutron-rich projectiles such as $^{48}$Ca and $^{72}$Zn systematically yield larger values of $C_{Q_{gg}}$ for a given fragment charge, indicating an enhanced production probability of neutron-rich fragments. This observation confirms that the amplitude parameter $C_{Q_{gg}}$ is sensitive not only to the fragment charge but also to the neutron content of the projectile.

Figure 6(a) extends this analysis to proton- and deuteron-induced reactions on $^{238}$U targets at relativistic energies, as well as to fragmentation of $^{238}$U projectiles. Although these reactions proceed via different initial mechanisms, the extracted values of $C_{Q_{gg}}$ are found to be compatible with the general systematics observed for heavy-ion-induced fragmentation. This result suggests that the $Q_{gg}$-based parameterization captures common features of fragment production that are largely independent of the entrance channel.

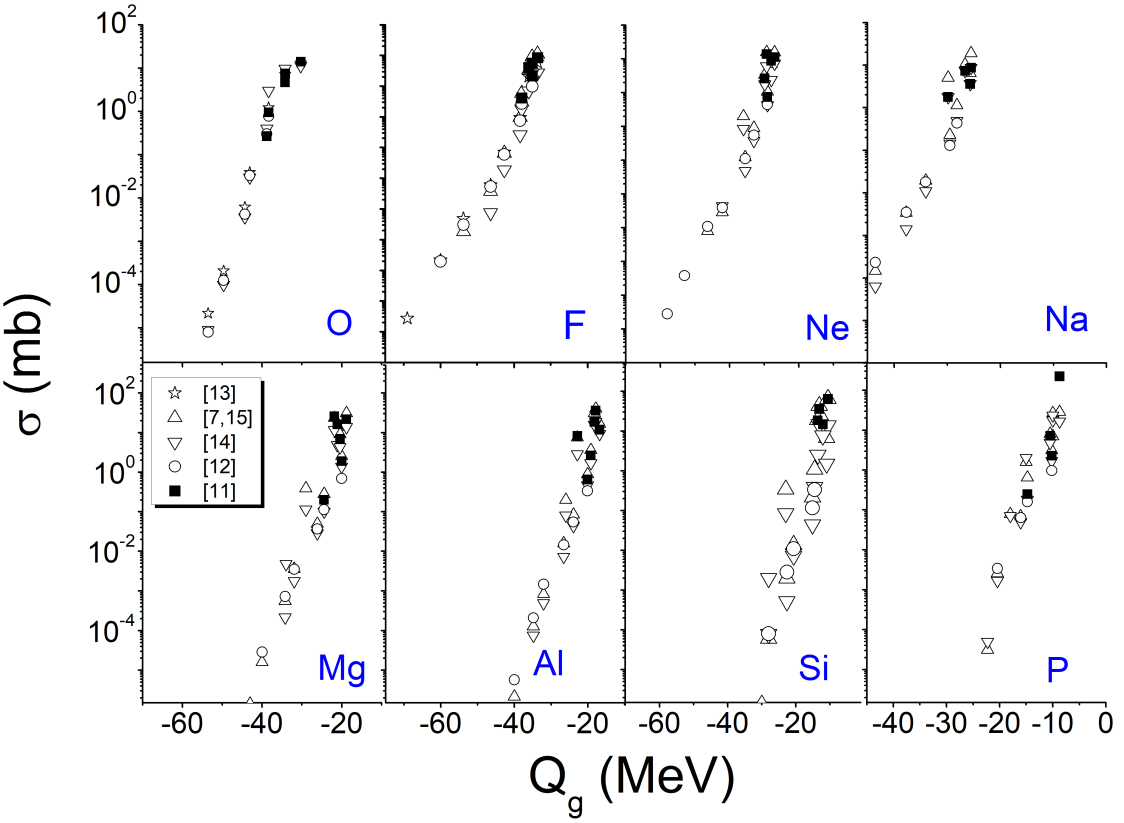


Figure 5: Production cross sections of O, F, Ne, Na, Mg, Al, Si, and P isotopes as functions of the $Q_{gg}$ value, obtained in projectile fragmentation of an Ar beam on a Be target at different energies: 35 MeV/nucleon [11], 57 MeV/nucleon [14], 90 MeV/nucleon [7, 15], 120 MeV/nucleon [12], and 1 GeV/nucleon [13].

Overall, the systematics presented in Figure 6 provide strong evidence that the parameter $C_{Q_{gg}}$ reflects fundamental properties of the fragment formation process and depends primarily on the fragment charge $Z$ and the neutron-to-proton ratio of the projectile. Together with the observed exponential dependence of the cross sections on $Q_{gg}$, this supports the applicability of the $Q_{gg}$ systematics as a unifying framework for describing the production of neutron-rich nuclei in fragmentation and transfer-like reactions.

Figure 7 shows the dependence of the parameter $\tau_{Q_{gg}}$ on the atomic number $Z$ of the detected fragments for a wide set of reactions induced by heavy ions, as well as by protons and deuterons at relativistic energies. The results are presented separately for reactions induced by heavy-ion projectiles and for reactions involving uranium targets or projectiles at high energies.

As can be seen from Figure 7(b), for fragmentation reactions induced by $^{40}$Ar, $^{48}$Ca, and $^{58,64}$Ni projectiles on Be and Ta targets, the parameter $\tau_{Q_{gg}}$ exhibits a nonmonotonic dependence on $Z$. In the region of intermediate fragment charges ($Z \approx 12$–$20$), a pronounced local maximum is observed, followed by a decrease of $\tau_{Q_{gg}}$ for heavier fragments. This behavior is systematically reproduced for different projectiles and target combinations, indicating that it reflects an intrinsic property of the fragment formation process rather than experimental uncertainties.

A similar trend is observed in Figure 7(a) for reactions induced by heavier

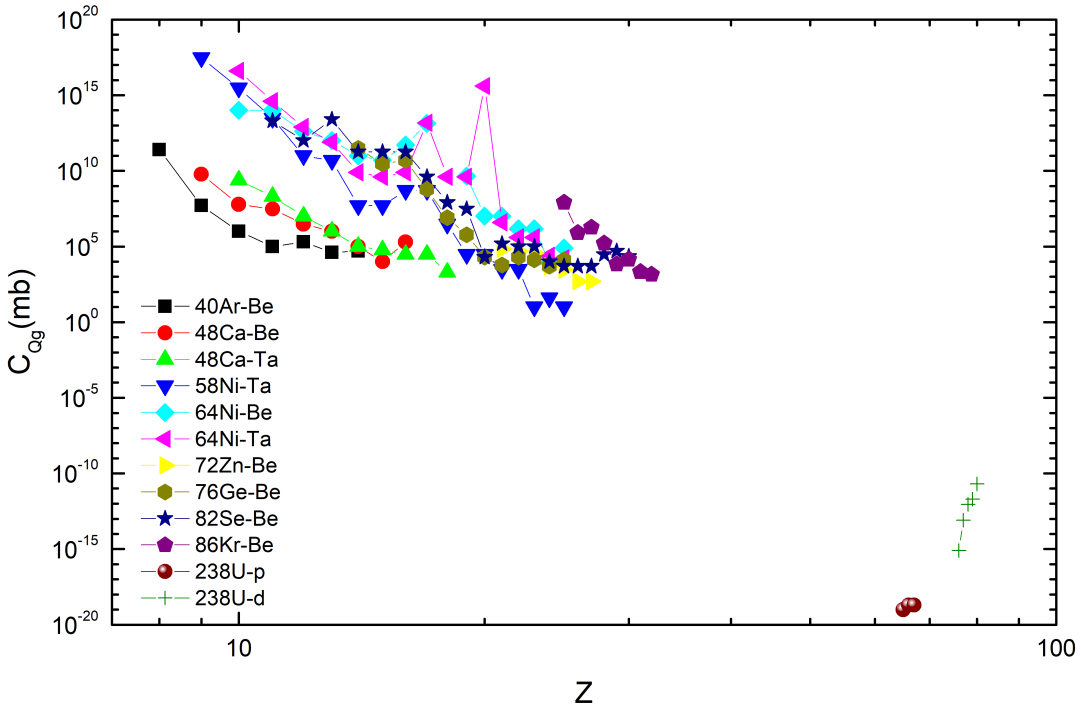


Figure 6: Dependence of the fitting parameter $C_{Q_{gg}}$ on the atomic number $Z$ of the detected fragments for various reactions. Shown are results for $^{58}$Ni+Ta and $^{64}$Ni+Be [19], $^{48}$Ca+Ta and $^{48}$Ca+Be [19], $^{40}$Ar+Be [11], and $^{86}$Kr+Be [19]. Also included are data obtained with secondary beams in the reactions $^{68}$Ni+Be and $^{72}$Zn+Be [20], as well as results for proton- and deuteron-induced reactions on U targets at relativistic energies [2], and for the reaction $^{76}$Ge+Be at 132 MeV/nucleon [5].

projectiles such as $^{72}$Zn, $^{76,82}$Ge, and $^{86}$Kr, as well as for proton- and deuteron-induced reactions on $^{238}$U targets. Despite the significant differences in entrance channels and reaction energies, the extracted values of $\tau_{Q_{gg}}$ fall within a relatively narrow range, typically between 1 and 2.5 MeV, and show comparable variations with fragment charge. This suggests that the parameter $\tau_{Q_{gg}}$ reflects an effective slope characterizing the statistical population of final fragments and is only weakly dependent on the specific reaction mechanism.

The presence of a local maximum in $\tau_{Q_{gg}}(Z)$ for fragments with $Z > 20$, observed most clearly for Ni-induced reactions, correlates with a similar feature found in the $C_{Q_{gg}}(Z)$ systematics. This correlation indicates that both parameters are influenced by the same underlying physical factors, such as shell effects and changes in the excitation and de-excitation dynamics of the prefragments.

While both $Q_{gg}$- and BE/$A$-based systematics provide an exponential description of neutron-rich fragment yields, the BE/$A$ approach has the advantage of being independent of the masses of unobserved reaction partners and relies solely on properties of the detected fragments.

Overall, the systematics of $\tau_{Q_{gg}}$ presented in Figure 7 demonstrate that the $Q_{gg}$-based description provides a consistent and physically meaningful characterization of neutron-rich fragment production over a wide range of projectiles, targets, and energies. Together with the observed behavior of the amplitude parameter $C_{Q_{gg}}$, these results support the applicability of the $Q_{gg}$ systematics as a complementary

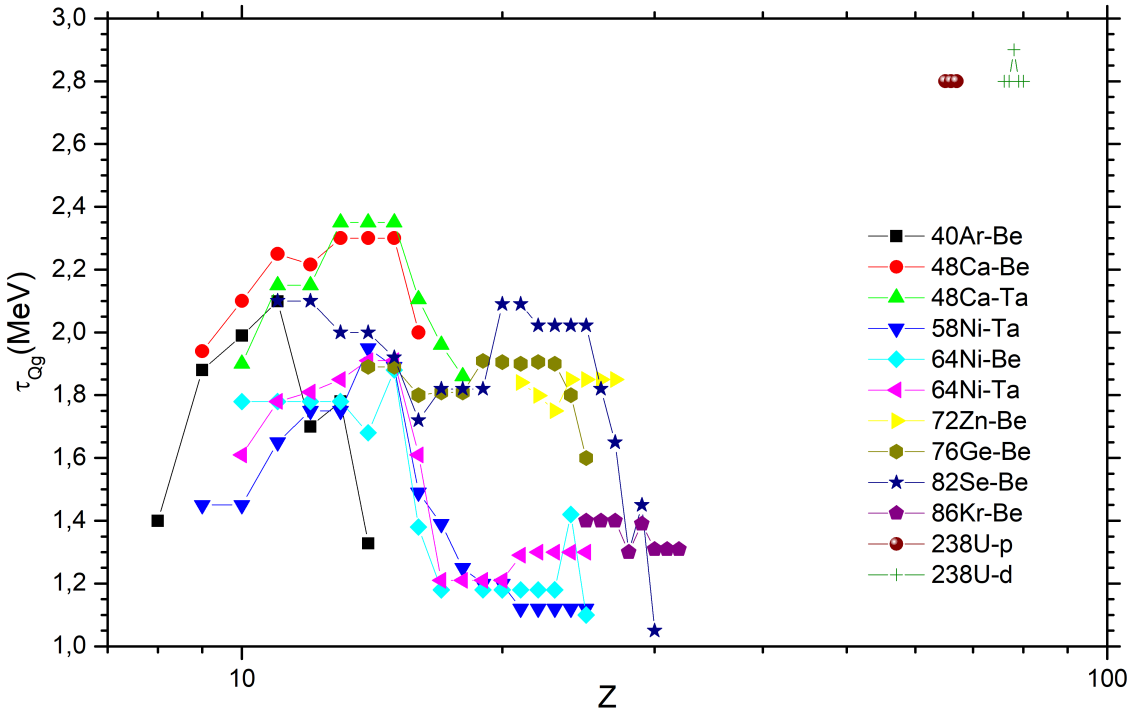


Figure 7: Dependence of the fitting parameter $\tau_{Q_{gg}}$ on the atomic number $Z$ of the detected fragments for various reactions. Shown are results for $^{58}$Ni+Ta and $^{64}$Ni+Be [19], $^{48}$Ca+Ta and $^{48}$Ca+Be [19], $^{40}$Ar+Be [11], and $^{86}$Kr+Be [19]. Also included are data obtained with secondary beams in the reactions $^{68}$Ni+Be and $^{72}$Zn+Be [20], as well as results for proton- and deuteron-induced reactions on U targets at relativistic energies [2], and for the reaction $^{76}$Ge+Be at 132 MeV/nucleon [5].

approach to the binding-energy-based description of fragmentation cross sections.

At the same time, it should be emphasized that the practical applicability of the $Q_{gg}$ systematics is limited by its explicit dependence on the masses of both the detected fragments and the unobserved reaction partners. In fragmentation and transfer-like processes involving highly excited prefragments, the effective reaction $Q$ values may be influenced by sequential particle emission and by uncertainties in the masses of nuclei far from stability. As a result, the use of $Q_{gg}$ -based parameterizations for extrapolations toward extremely neutron-rich nuclei may become model dependent. In this respect, systematics formulated in terms of the binding energy per nucleon of the final fragments offers a more robust and transparent framework, as it relies solely on intrinsic properties of the observed nuclei and avoids assumptions about unmeasured reaction channels.

# 5 Conclusions

An analysis of published zero-degree experimental data demonstrates that, within experimental uncertainties, the production cross sections of neutron-rich fragments in projectile fragmentation reactions are approximately independent of the incident projectile energy over a wide range from 35 MeV/nucleon up to 1 GeV/nucleon. This result provides direct experimental evidence for the limiting-fragmentation behavior extending well beyond the energy interval typically considered in earlier studies.

Based on this observation, an empirical systematics for neutron-rich fragment production has been formulated in terms of the binding energy per nucleon ( BE/$A$ ) of the final nuclei. The fragment yields follow a steep exponential dependence on BE/$A$ , spanning several orders of magnitude, with parameters that exhibit regular correlations with the fragment charge and the neutron-to-proton ratio of the projectile. The proposed BE/$A$-based systematics offers a simple and robust framework for describing and extrapolating fragmentation yields and provides a practical tool for estimating production cross sections of neutron-rich nuclei in future radioactive-beam experiments. The observed universality of the fragment yields implies that the dependence on the incident projectile energy becomes secondary once fragmentation occurs, while intrinsic nuclear-structure properties, as reflected by the binding energy per nucleon, play the dominant role in determining neutron-rich fragment production.

# References


[1] V. V. Volkov, *Treatise on Heavy-Ion Science*, Ed. D. A. Bromley, Plenum Press, Vol. 8, 101 (1989).

[2] G. D. Westfall *et al.*, Phys. Rev. C **17**, 1368 (1978).

[3] D. Guillemaud-Mueller, Yu. E. Penionzhkevich *et al.*, Z. Phys. A **332**, 189 (1989).

[4] D. Guillemaud-Mueller *et al.*, Phys. Rev. C **41**, 937 (1990).

[5] O. Tarasov *et al.*, Phys. Rev. C **80**, 034609 (2009).

[6] O. Tarasov *et al.*, Phys. Rev. C **87**, 054612 (2013).

[7] M. Notani, Phys. Rev. C **76**, 044605 (2007).

[8] K. Summerer *et al.*, Phys. Rev. C **61**, 034607 (2000).

[9] T. Baumann *et al.*, Nature **449**, 1022 (2007).

[10] G. G. Adamian *et al.*, Phys. Rev. C **78**, 024613 (2008).

[11] Yu. Sereda, S. Lukyanov, Yad. Fiz. **77**, 864 (2014).

[12] E. Kwan *et al.*, Phys. Rev. C **86**, 014612 (2012).

[13] A. Ozawa *et al.*, Nucl. Phys. A **673**, 411 (2000).

[14] X. H. Zhang *et al.*, Phys. Rev. C **85**, 024621 (2012).

[15] S. Momota *et al.*, Nucl. Phys. A **701**, 150 (2002).

[16] M. Mocko *et al.*, Europhys. Lett. **79**, 12001 (2007).

[17] B. M. Tsang *et al.*, Phys. Rev. C **76**, 041302(R) (2007).

[18] G. Chaudhuri *et al.*, Phys. Rev. C **76**, 067601 (2007).

[19] M. Mocko *et al.*, Phys. Rev. C **76**, 014609 (2007).

[20] S. Lukyanov *et al.*, Phys. Rev. C **80**, 014609 (2009).

[21] C.-W. Ma *et al.*, Prog. Part. Nucl. Phys. **121**, 103911 (2021).

[22] J. M. Boillos *et al.*, Phys. Rev. C **105**, 014611 (2022).

[23] B. Mei *et al.*, Phys. Rev. C **108**, 034602 (2023).

[24] N. Tang *et al.*, Phys. Rev. C **107**, 014603 (2023).

[25] P. Feng *et al.*, Phys. Rev. C **111**, 024603 (2025).